SUPPLEMENTARY FIGURES (Figures S1 – S13)

Activation of Viral Transcription by Stepwise Largescale Folding of an RNA Virus Genome

Tamari Chkuaseli and K. Andrew White

Department of Biology, York University, Toronto, Ontario, Canada M3J 1P3

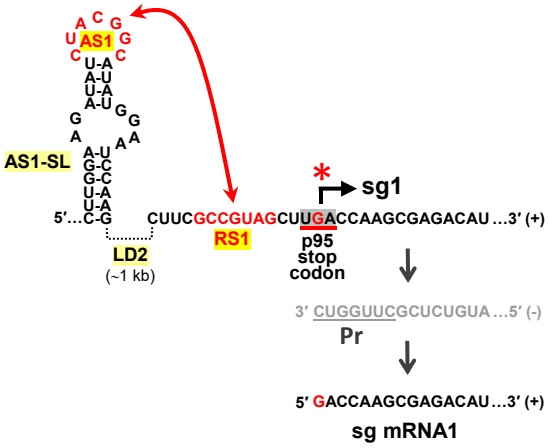

Figure S1. Detailed depiction of the AS1 and RS1 RNA elements in CIRV that activate sg mRNA1 transcription. AS1 and RS1 are shown in red, with AS1 positioned in the terminal loop of AS1-SL. The p95 stop codon (red underline) overlaps with the initiating nucleotide for sg mRNA1 transcription (red G). The truncated minus-strand RNA intermediate synthesized during sg mRNA1 transcription is shown in grey nucleotides, with the promoter (Pr) sequence underlined. The minus-strand intermediate is generated when the RdRp encounters the AS1/RS1 stem in the genome, which causes it to terminate synthesis. The 3′-truncated minus-strand generated then serves as a template for transcription of sg mRNA1.

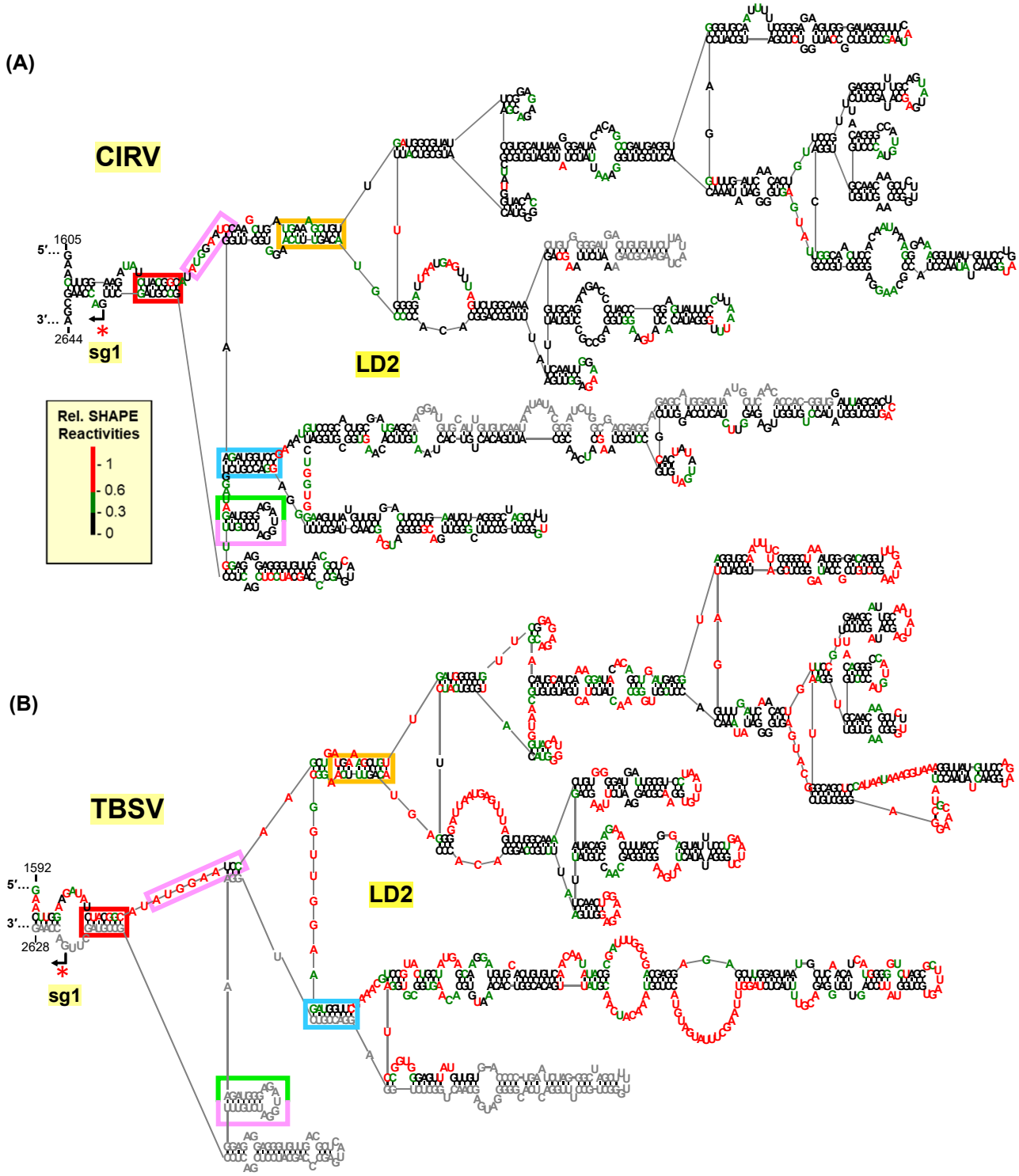

Figure S2. RNA secondary structure of LD2 in the CIRV genome deduced through selective 2'-hydroxyl acylation analyzed by primer extension (SHAPE). (A) SHAPE analysis was performed on the full-length CIRV RNA genome. The averages of normalized SHAPE reactivities from two independent SHAPE experiments were used as folding constraints in *RNAstructure* (slope value = 1.8 kcal/mol and intercept value = -0.6 kcal/mol) to deduce an RNA secondary structure for LD2. Nucleotides coloured in red were highly reactive, in green were moderately reactive, and in black were weakly reactive or unreactive. Nucleotides in grey correspond to regions for which no SHAPE data was obtained. **(B)** For comparison, SHAPE-guided secondary structure of LD2 in TBSV (adapted from 48). Key corresponding structural features are colour-coded (see text for details).

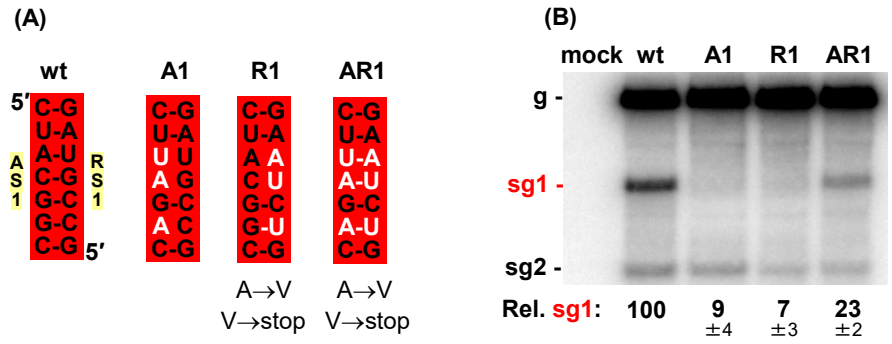

Figure S3. The AS1/RS1 LDRI regulates sg mRNA1 transcription in CIRV. (A) Compensatory mutations introduced in AS1 and RS1 in CIRV are shown in white. Amino acid changes in p95 are indicated under the mutant sequences. **(B)** Northern blot analysis of plus-strand CIRV RNAs extracted from protoplasts transfected with wt and mutant CIRV genomic RNAs shown in panel (A). Identities of the tested genomes are indicated above the blot, and positions of CIRV genome (g) and subgenomic mRNAs (sg1 and sg2) are shown on the left. Average plus-strand sg mRNA1 accumulation levels relative to that of the wt are provided below the blot with standard errors obtained from three independent experiments.

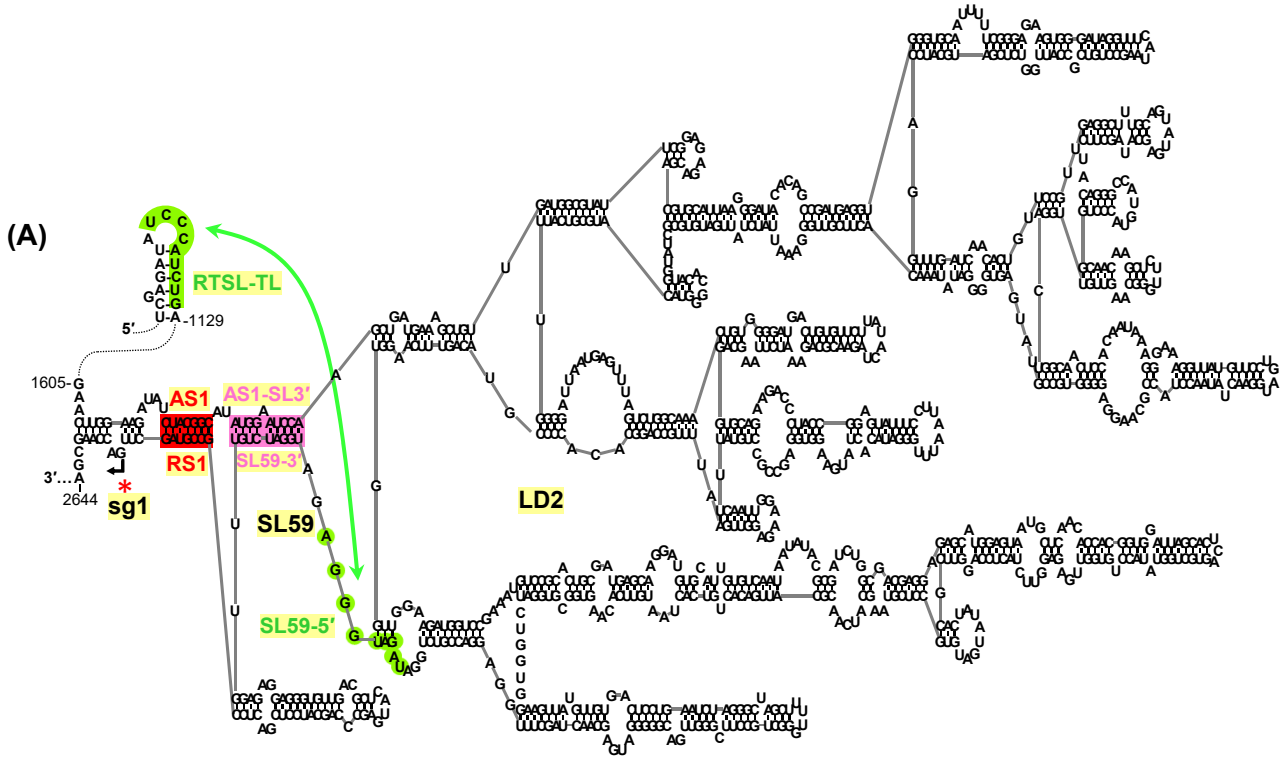

(B)

	AS1	RS1	AS1-SL3′	SL59-3′	RTSL-TL	SL59-5′
CIRV	5′…CUACGGC…3′	5′…GCCGUAG…3′	5′…AUGGAAUCCA…3′	5′…UGGAUCUGU…3′	5′…UCCCAUCUG…3′	5′…UAGAUGGGA…3′
LNV	…CUGCGGC…	…GCCGUAG…	…AUGGAGCUCCA…	…UGGACCUAU…	…UCCCAUCUG…	…UAGAUGGGA…
PLV	…CUGCGGC…	…GCCGUGG…	…AUGGAGCUCCA…	…UGGACCUAU…	…UCCCAUCUG…	…UAGAUGGGA…
TBSV-Ch	…CUACGGC…	…GCCGUAG…	…AUGGAAUCCA…	…UGGAUCUGU…	…UCCCAUCUG…	…AAGAUGGGA…
TBSV-P	…CUACGGC…	…GCCGUAG…	…AUGGAAUCCA…	…UGGAUCUAU…	…UCCCAUCUG…	…GAGAUGGGA…
AMCV	…CUACGGC…	…GCCGUAG…	…AUGGAAUCCA…	…UGGAUUUGU…	…UCCCAUCUG…	…UAGAUGGGA…
TBSV-Nf	…CUACGGC…	…GCCGUAG…	…AUGGAAUCCA…	…UGGAUUUAU…	…UCCCAUCUG…	…UAGAUGGGA…
TBSV-St	…CUGCGGC…	…GCCGUAG…	…AUGGAAUCCA…	…UGGAUCUAU…	…UCCCAUCUG…	…UAGAUGGGA…
GALV	…CUGCGGC…	…GCCGUAG…	…AUGGAAUCCA…	…UGGAUCUGU…	…UCCCAUCUG…	…UAGGUGGGA…
PNSV	…CUACGGC…	…GCCGUGG…	…AUGGAAUCCA…	…UGGAUCUAU…	…UCCCAUCUG…	…CAGAUGGGA…
CuNV	…CUGCGGC…	…GCCGUAG…	…AUGGAAUCCA…	…UGGAUCUUU…	…UCCCAUCUG…	…CAGAUGGGA…
CymRV	…CUACGGC…	…GCCGUAG…	…AUGGAAUCCA…	…UGGAUCUAU…	…UCCCAUCUG…	…UAGAUGGGA…
CBLV	…CUGCGGC…	…GCCCCAG…	…UUGGAGAGUA…	…UGGAUCUCU…	…UCCCAUCUG…	…CCGAUGGGA…
LNSV-L2	…CUACGGC…	…GCCGUAG…	…AUGGAAUCCA…	…UGGAUCUAU…	…UCCCAUCUG…	…CAGAUGGGA…
MPV-PM75	…CUACGGC…	…GCCGUAG…	…AUGGAAUCCA…	…UGGAUCUAU…	…UCCCAUCUG…	…CAGAUGGGA…
EMCV	…CUGCGGC…	…GCCGUAG…	…AUGGAGCUCCA…	…UGGACCUAU…	…UCCCACCUG…	…UAGAUGGGA…
CIRV-CZ	…CUGCGGC…	…GCCGUAG…	…AUGGAAUCCA…	…UGGAUCUAU…	…UCCCAUCUG…	…CAGGUGGGA…
PLCV-T46	…CUACGGC…	…GCCGUAG…	…AUGGAAUCCA…	…UGGAUCUAU…	…UCCCAUCUG…	…AAGAUGGGA…
MNeSV	…CUGCGGC…	…GCCCCAG…	…UUAGAGCUCCA…	…UGGACUUAU…	…UCCCAUCCCG…	…GAGAUGGGA…
	** ****	**** *	* ** *	**** * *	*********	* *****

CBLV – alternative interaction: …UUGGAGAGUA… …UGGAUCUCUUUGG…

Figure S4

Figure S4. Structural depiction and comparative sequence analysis of the AS1/RS1, AS1-SL3'/SL59-3', and RTSL-TL/SL59-5' interactions. (A) CIRV secondary structure showing formation of the intra-LD2 AS1-SL3'/SL59-3' (pink) interaction. **(B)** Comparative sequence analysis of AS1/RS1 (red), AS1-SL3'/SL59-3' (pink) and RTSL-TL/SL59-5' (green) interactions between the members of the Tombusvirus genus, and Zeavirus genus (*i.e.* MNeSV, the most closely related genus to tombusviruses). Nucleotide substitutions that maintain base pairing are in white, while those that do not preserve pairing are in red. The asterisks below correspond to the nucleotides that are 100% conserved. The AS1-SL3'/SL59-3' (pink) interaction for CBLV does not conform to the pairing scheme observed in the other viruses, and when the CBLV genome was analyzed by *mFold* an alternative base pairing scheme was predicted (boxed sequences at bottom of table). Tombusviruses: Carnation Italian ringspot virus (CIRV, NC_003500.3), Lisianthus necrosis virus (LNV, DQ011234.1), Pear latent virus (PLV, AY100482.1), Tomato bushy stunt virus cherry isolate (TBSV-Ch, M21958.1), TBSV pepper isolate (TBSV-P, U80935.1), Artichoke mottled crinkle virus (AMCV, NC_001339.1), TBSV nipplefruit isolate (TBSV-Nf, AY579432), TBSV statice isolate (TBSV-St, AJ249740.1), Grapevine Algerian latent virus (GALV, NC_011535.1), Pelargonium necrotic spot virus (PNSV, NC_005285.1), Cucumber necrosis virus (CuNV, NC_001469.1), Cymbidium ringspot virus (CymRSV, NC_003532.1), Cucumber Bulgarian latent virus (CBLV, NC_004725.1), Lettuce necrotic stunt virus isolate L2 (LNCV-L2, JN700748.1), Moroccan pepper virus isolate PM75 (MPV-PM75, NC_020073.2), Eggplant mottled crinkle virus (EMCV, NC_023339.1), CIRV isolate CZ (KP888563.1), Pelargonium leaf curl virus isolate T46 (PLCV-T46, NC_030452.1). Zeavirus: Maize necrotic streak virus (MNeSV, NC_007729.1).

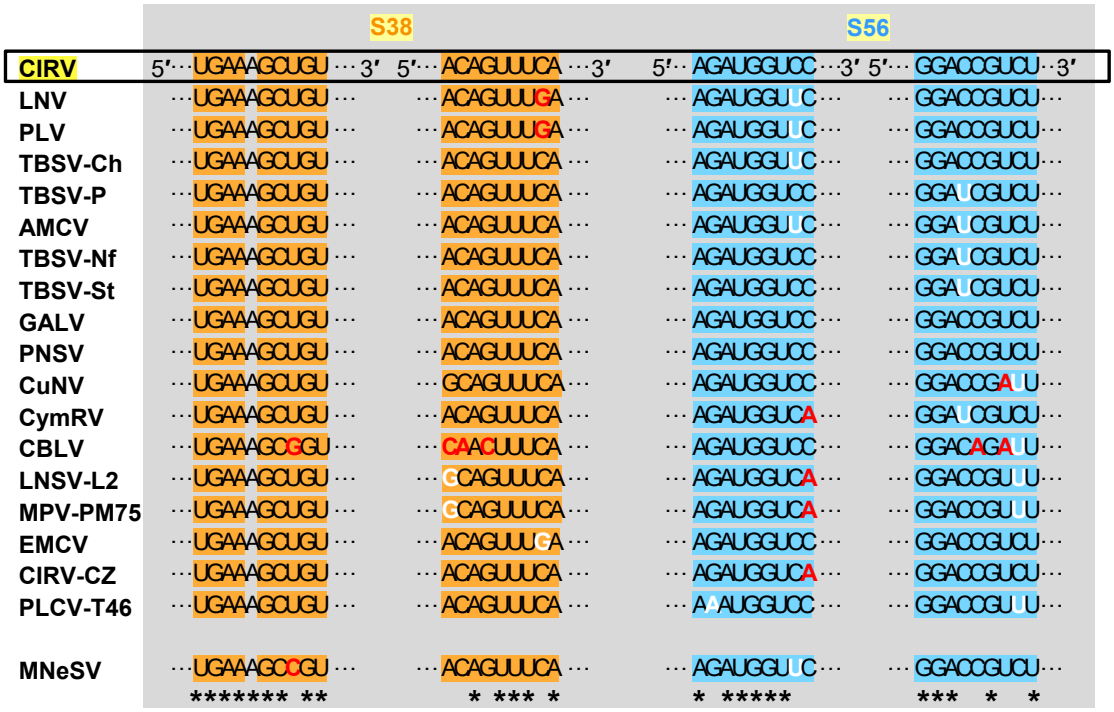

Figure S5. Comparative sequence analysis of S38 and S56 in the Tombusvirus and Zeavirus genera. Nucleotide substitutions that maintain base pairing are depicted in white, while those that do not preserve pairing are in red. The asterisks below correspond to the nucleotides that are 100% conserved among the analysed viral sequences. Tombusviruses: Carnation Italian ringspot virus (CIRV, NC_003500.3), Lisianthus necrosis virus (LNV, DQ011234.1), Pear latent virus (PLV, AY100482.1), Tomato bushy stunt virus cherry isolate (TBSV-Ch, M21958.1), TBSV pepper isolate (TBSV-P, U80935.1), Artichoke mottled crinkle virus (AMCV, NC_001339.1), TBSV nipplefruit isolate (TBSV-Nf, AY579432), TBSV statice isolate (TBSV-St, AJ249740.1), Grapevine Algerian latent virus (GALV, NC_011535.1), Pelargonium necrotic spot virus (PNSV, NC_005285.1), Cucumber necrosis virus (CuNV, NC_001469.1), Cymbidium ringspot virus (CymRSV, NC_003532.1), Cucumber Bulgarian latent virus (CBLV, NC_004725.1), Lettuce necrotic stunt virus isolate L2 (LNCV-L2, JN700748.1), Moroccan pepper virus isolate PM75 (MPV-PM75, NC_020073.2), Eggplant mottled crinkle virus (EMCV, NC_023339.1), CIRV isolate CZ (KP888563.1), Pelargonium leaf curl virus isolate T46 (PLCV-T46, NC_030452.1). Zeavirus: Maize necrotic streak virus (MNeSV, NC_007729.1).

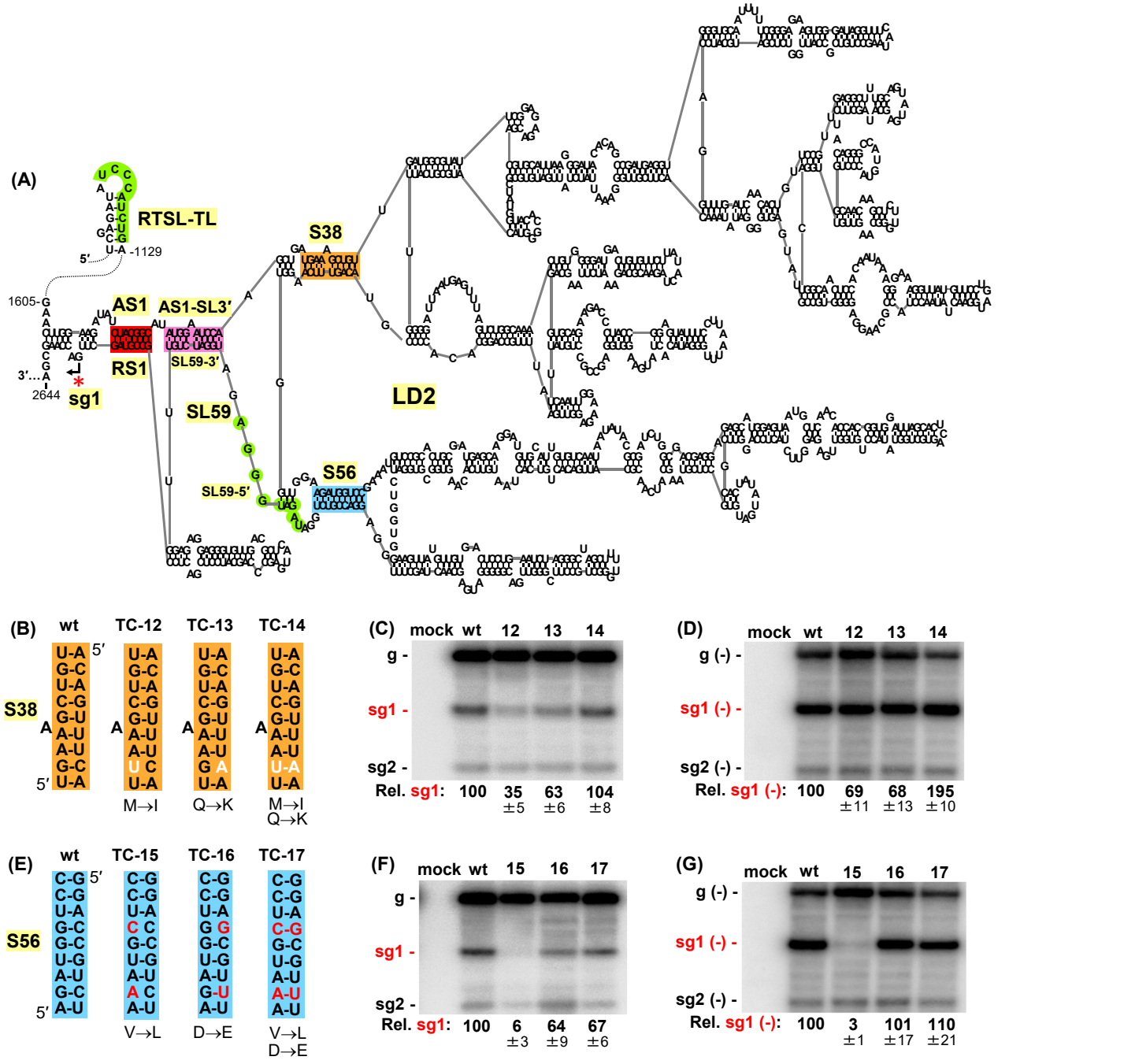

Figure S6. Functional analysis of S38 and S56. (A) Secondary structure of RTSL-TL and LD2 regions in the CIRV genome. Key structures are colour-coded. **(B)**, **(E)** Compensatory substitutions that were introduced in the full-length CIRV genome to functionally assess S38 (orange) and S56 (blue), respectively. Amino acid changes in the p95 ORF are indicated under each mutant. **(C)**, **(F)** Northern blot analysis of plus-strand RNAs isolated from protoplasts transfected with CIRV wt and mutant genomic RNAs shown in (B) and (E), respectively. Identities of the tested samples are indicated above the blots and positions of positive-sense genome and sg mRNAs are shown on the left. Average sg mRNA1 accumulation levels relative to that of the wt are provided below the blots with standard errors obtained from three independent experiments. **(D)**, **(G)** Northern blot analysis of minus-strand CIRV RNAs isolated from protoplast infections. Average minus-strand sg mRNA1 accumulation levels relative to that of the wt are provided below the blots with standard errors obtained from three independent experiments. For mutant 12 in panel D and mutant 16 in panel G, relative sg RNA minus-strand levels were higher than their plus-strand counterparts. This is likely due to inaccurate RdRp termination (caused by a mutated attenuation structure) during (-)sgRNA synthesis, which results in a promoter (Pr, see supplemental Fig. S1) with either missing or added 3′-terminal nucleotides that inhibits its use as transcriptional promoter.

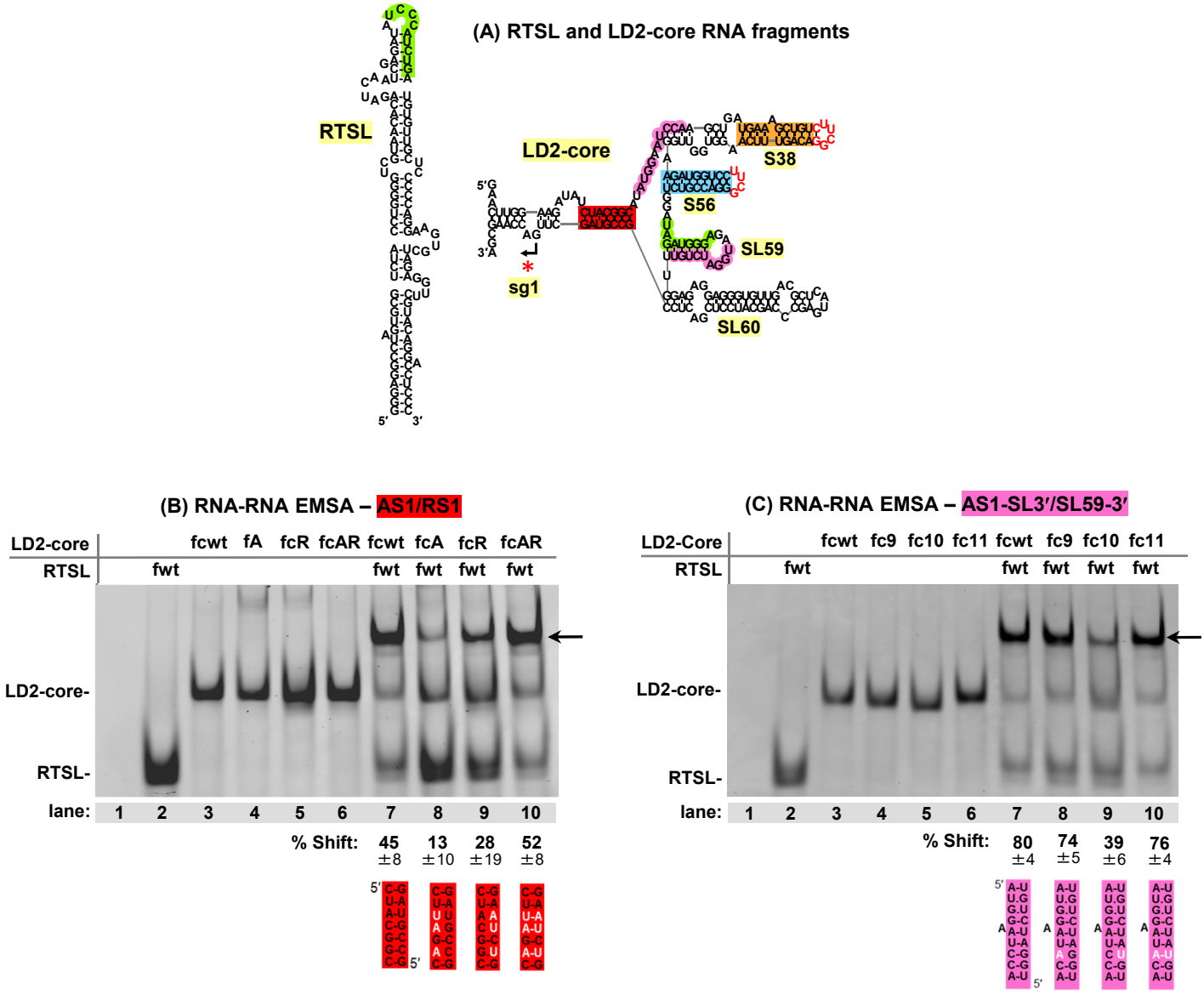

Figure S7. RTSL/LD2-core complex formation relies on both the AS1/RS1 and AS1-SL3'/SL59-3' interactions. (A) Secondary structures of RTSL (106 nt) and LD2-core (188 nt) RNA fragments tested in RNA-RNA EMSAs. RTSL-TL (green), AS1/RS1 (red), AS1-SL3' (pink), S38 (orange), S56 (blue), SL59 (green and pink), and LS60 are indicated. Sg mRNA1 initiation site is depicted with a small black arrow and a red asterisk. **(B)**, **(C)** RNA-RNA EMSA results for RTSL and LD2-core RNA fragments shown in panel (A) with the modifications indicated below the gels. RNAs were separated in native 8% polyacrylamide gels, which were stained with ethidium bromide. The contents of each lane are indicated above the gels with the fragment type shown to the far left. Lane 1 contains only RNA binding buffer and glycerol. The black arrows on the right side of the images point to where the RTSL/LD2-core complexes migrate. The percentages and standard errors of shifted LD2-core RNAs compared to the corresponding non-shifted LD2-core RNAs are displayed below the gels and were obtained from three independent EMSA experiments.

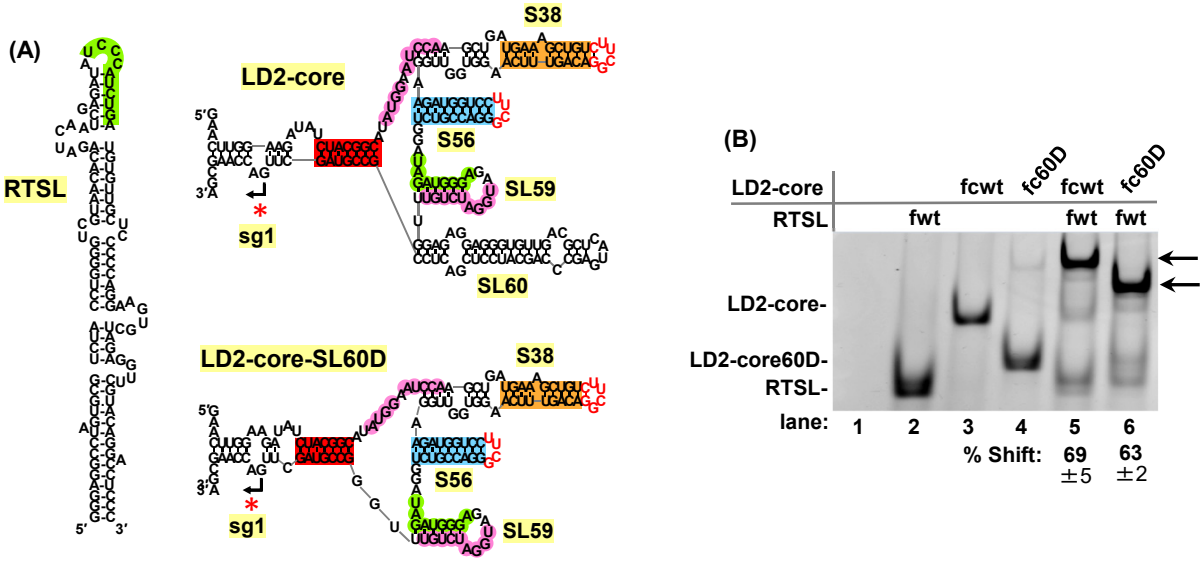

Figure S8. SL60 is not required for RTSL/LD2-core complex formation. (A) RNA secondary structures of RTSL (106 nt), LD2-core (188 nt), and LD2-core-SL60D (145 nt, with SL60 deleted) fragments tested by RNA-RNA EMSA. **(B)** RNA-RNA EMSA results for the RNA fragments shown in (A). The contents of each lane are indicated above the native 8% polyacrylamide gel stained with ethidium bromide, with the fragment type shown on the far left. Lane 1 represents a mock lane containing only RNA binding buffer and glycerol. The black arrows on the right side of the image point to where the RTSL/LD2-core and RTSL/LD2-core-SL60D complexes migrate. The percentages and standard errors of shifted LD2-core RNAs compared to the corresponding non-shifted LD2-core RNAs are displayed below the gels and were obtained from three independent EMSA experiments.

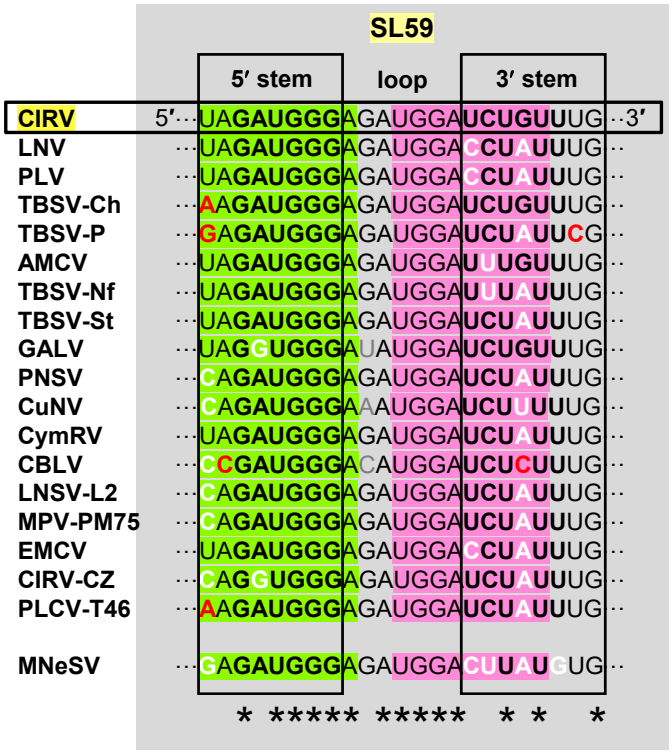

Figure S9. Comparative sequence analysis of SL59 in the Tombusvirus and Zeavirus genera. Boxed nucleotides represent complementary sequences that form the stem of SL59. The green and pink nucleotides depict SL59-5' and AS1-SL3' sequences that are complementary to RTSL-TL and AS1-SL3' sequences, respectively. Nucleotide substitutions that maintain base pairing are in white, while those that do not preserve pairing are in red. The asterisks below correspond to the nucleotides that are 100% conserved. Tombusviruses: Carnation Italian ringspot virus (CIRV, NC_003500.3), Lisianthus necrosis virus (LNV, DQ011234.1), Pear latent virus (PLV, AY100482.1), Tomato bushy stunt virus cherry isolate (TBSV-Ch, M21958.1), TBSV pepper isolate (TBSV-P, U80935.1), Artichoke mottled crinkle virus (AMCV, NC_001339.1), TBSV nipplefruit isolate (TBSV-Nf, AY579432), TBSV statice isolate (TBSV-St, AJ249740.1), Grapevine Algerian latent virus (GALV, NC_011535.1), Pelargonium necrotic spot virus (PNSV, NC_005285.1), Cucumber necrosis virus (CuNV, NC_001469.1), Cymbidium ringspot virus (CymRSV, NC_003532.1), Cucumber Bulgarian latent virus (CBLV, NC_004725.1), Lettuce necrotic stunt virus isolate L2 (LNCV-L2, JN700748.1), Moroccan pepper virus isolate PM75 (MPV-PM75, NC_020073.2), Eggplant mottled crinkle virus (EMCV, NC_023339.1), CIRV isolate CZ (KP888563.1), Pelargonium leaf curl virus isolate T46 (PLCV-T46, NC_030452.1). Zeavirus: Maize necrotic streak virus (MNeSV, NC_007729.1).

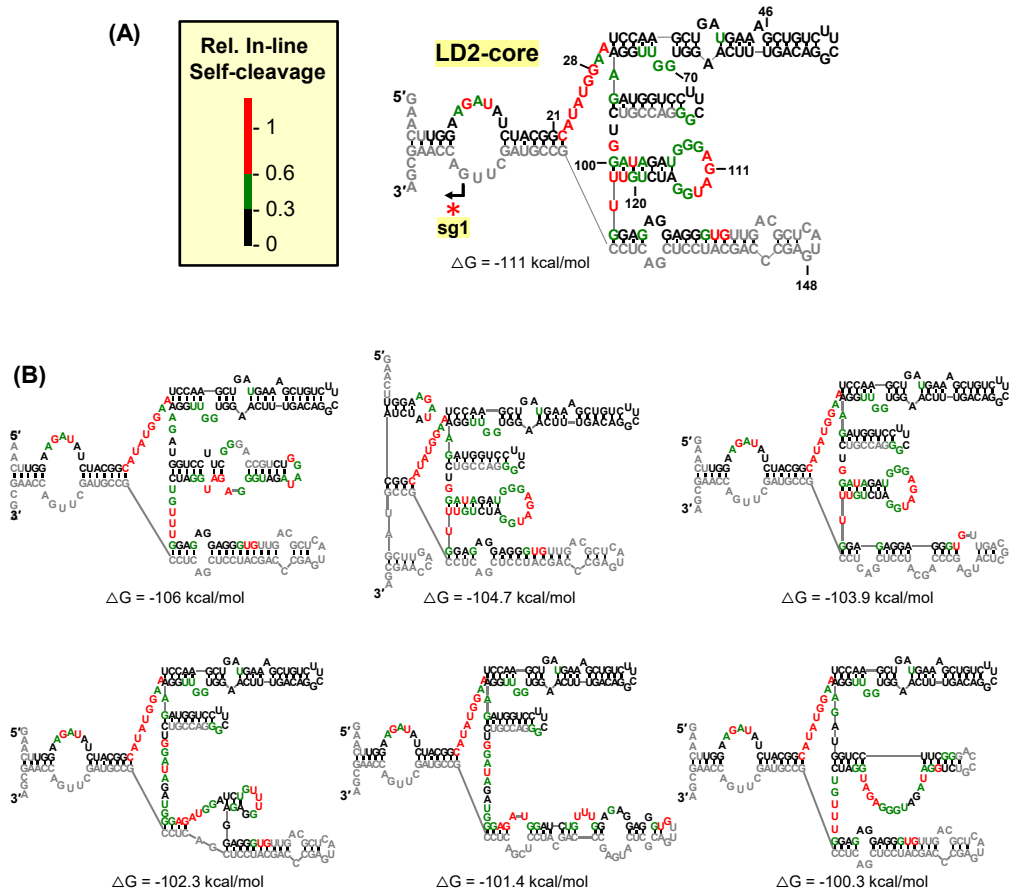

(C) **LD2-core** (free)

Nucleotide Position	Relative Self-cleavage Levels
1	
⋮	
6	0.040040646
7	0.03515452
8	0.045114822
9	0.058427861
10	0.392942868
11	7.609050702
12	0.316103884
13	1.322596846
14	0.057581272
15	0.0978398
16	0.030831967
17	0.078571861
18	0.015884511
19	0.026641631
20	0.028344097
21	0.067648945
22	0.608071555
23	1.256700119
24	1.28850328
25	0.952249121
26	1.250727204
27	1.282791756
28	0.755831877
29	0.39196196
30	0.601232828
31	0.120207651
32	0.052005275
33	0.06856054
34	0.144956913
35	0.163907352
36	0.069895001
37	0.044261757
38	0.068727743
39	0.059825054
40	0.131817132
41	0.500915033
42	0.119450034
43	0.122159585
44	0.135530505
45	0.265524221
46	0.126033583
47	0.023026281
48	0.018163751
49	0.008363368
50	0.007977678
51	0.008150851
52	0.011071323
53	0.034372167
54	0.027644828
55	0.024532527
56	0.008492562
57	0.01052237
58	0.021023791
59	0.017607648
60	0.01775595
61	0.018715794
62	0.028279951
63	0.052278867
64	0.072441533
65	0.112018445
66	0.090650356
67	0.114595522
68	0.21537867
69	0.29762994
70	0.473021657
71	0.486586091
72	0.458656859
73	0.320926827
74	0.278096687
75	0.233592283
76	0.276041193
77	0.331253323
78	0.345518189
79	0.151356442
80	0.144029298
81	0.073911609
82	0.060491121
83	0.065710792
84	0.068131652
85	0.061910728
86	0.066709512
87	0.104327843
88	0.1715945
89	0.36423537
90	0.398896246
⋮	
97	0.109499439
98	0.239826449
99	0.685358783
100	0.495289192
101	0.508191516
102	0.726523823
103	0.463966552
104	0.259090554
105	0.285351337
106	0.337929429
107	0.350208813
108	0.418854725
109	0.496571309
110	0.61071755
111	0.768571111
112	0.851467171
113	0.866634537
114	0.481567292
115	0.339172218
116	0.235600272
117	0.18348433
118	0.200666561
119	0.300627662
120	0.544912081
121	0.910791629
122	1.89226667
123	2.490116776
124	0.516867829
125	0.17459244
126	0.183243381
127	0.376783691
128	0.254370437
129	0.100060882
130	0.051306745
131	0.036506825
132	0.118011955
133	0.171852158
134	0.304033532
135	0.936825274
136	1.726774857
⋮	
188	

Figure S10. **RNA secondary structure for the free CIRV LD2-core deduced from in-line probing. (A)** LD2-core secondary structure with nucleotides coloured according to their relative in-line cleavage values, with red being frequently cleaved, green, cleaved at intermediate frequency, and black, infrequently cleaved. Nucleotides in grey represent the areas were relative in-line values could not be determined. The optimal secondary structure was obtained by inputting the relative in-line probing values into the *RNAstructure* web server to generate an in-line-guided structural model for LD2-core. The quantification of the in-line probing data was obtained by determining the intensity of each band in the lane containing free LD2-core RNA (Figure 7A, lane 4) using the QuantityOne (Biorad) software, with background level subtracted. The value for each band was normalized relative to the average value for top ten highest values. The normalized values were then used as folding constraints in *RNAstructure* web server with slope value set to 1.8 kcal/mol and intercept value set to -0.6 kcal/mol. **(B)** Suboptimal secondary structure predictions of LD2-core, within 10% of the optimal structure, using the in-line constraints as described above. **(C)** A table showing nucleotide positions and their corresponding normalized in-line reactivity values. Values for nucleotides 1-5, 91-96, as well as, 137-188 could not be quantified. The relative in-line values are colour-coded according to the scale shown in panel (A).

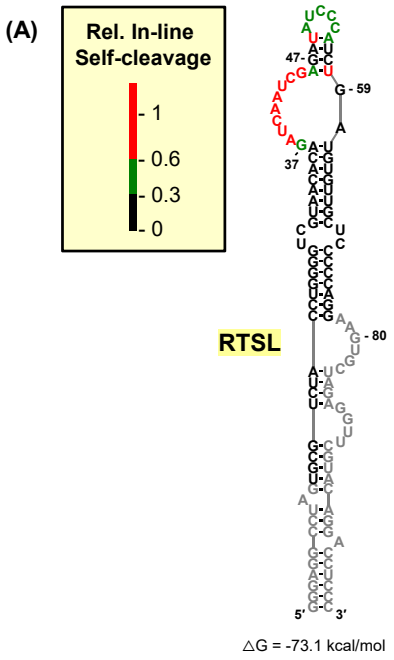

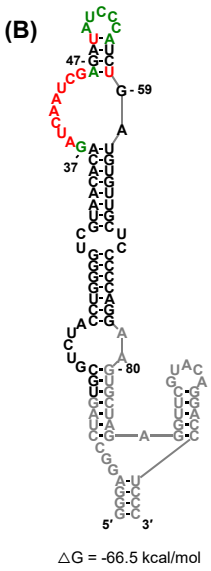

(C) RTSL (free)

Nucleotide Position	Relative Self-cleavage Levels
1	
⋮	
12	0.032174798
13	0.048571818
14	0.092572552
15	0.265122695
16	0.242744463
17	0.204024133
18	0.24169773
19	0.220472326
20	0.063513145
21	0.078613681
22	0.052566625
23	0.142214006
24	0.093279343
25	0.081848904
26	0.182420835
27	0.070370122
28	0.085911526
29	0.067887161
30	0.073947621
31	0.047883458
32	0.041017762
33	0.039472058
34	0.036411826
35	0.074207204
36	0.22650011
37	0.530208873
38	0.863890425
39	1.685503084
40	1.607062511
41	0.867800386
42	0.770018883
43	0.909028779
44	0.926480769
45	1.053048178
46	0.382909194
47	0.212275249
48	0.28265575
49	0.699509977
50	0.997987724
51	0.489659562
52	0.44700461
53	0.593803801
54	0.540372313
55	0.343671719
56	0.218472353
57	0.252114337
58	0.618886598
59	0.253703607
60	0.237210128
61	0.180344905
62	0.14576307
63	0.140598662
64	0.14876417
65	0.139807313
66	0.094979323
67	0.149709286
68	0.192952415
69	0.11782957
70	0.082312072
71	0.055572344
72	0.04215052
73	0.041954368
74	0.059783675
75	0.067494974
76	0.081995281
77	0.168993896
⋮	
106	

Figure S11. **RNA secondary structure for the free CIRV RTSL determined from in-line probing analysis. (A)** RTSL secondary structure with nucleotides coloured according to their relative in-line cleavage values, with red being frequently cleaved, green, cleaved at intermediate frequency, and black, infrequently cleaved. Nucleotides in grey represent the areas were relative in-line values could not be determined. The secondary structure was determined by inputting the relative in-line probing values into the *RNAstructure* web server to generate an in-line-guided structural model for RTSL. To obtain the relative in-line probing data the intensity of each band in the lane containing free RTSL RNA (Figure 7C, lane 4) was quantified using the QuantityOne (Biorad) software, with background level subtracted. The value for each band was normalized relative to the average value for top ten highest values. The normalized values were then used as folding constraints in *RNAstructure* web server with slope value set to 1.8 kcal/mol and intercept value set to -0.6 kcal/mol. **(B)** A suboptimal secondary structure of RTSL, within 10% of the optimal structure, predicted through using in-line constraints as described above. **(C)** A table showing nucleotide positions and their corresponding normalized in-line reactivity values. Values for nucleotides 1-11 and 78-106 could not be quantified. The relative in-line values are colour-coded according to the scale shown in panel (A).

(A)

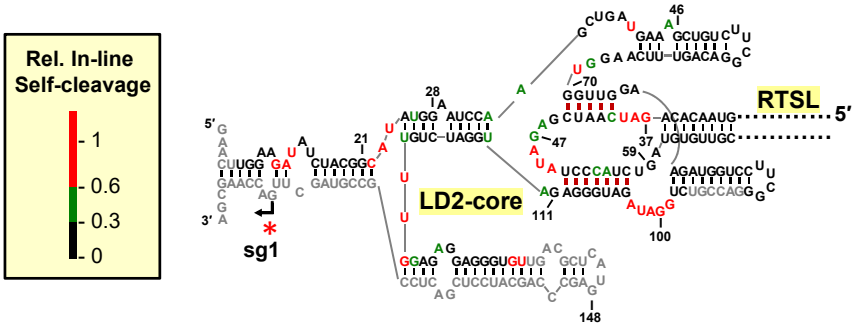

(B) RTSL (complexed)

Nucleotide Position	Relative Self-cleavage Levels
1	
⋮	
12	0.023553
13	0.028482
14	0.093097
15	0.286619
16	0.242127
17	0.216130
18	0.239524
19	0.199685
20	0.043011
21	0.061902
22	0.051894
23	0.156932
24	0.089903
25	0.082613
26	0.198506
27	0.058691
28	0.106066
29	0.066709
30	0.073593
31	0.036710
32	0.027699
33	0.017375
34	0.018316
35	0.054870
36	0.147941
37	0.860360
38	1.874950
39	1.638648
40	0.329944
41	0.205065
42	0.196099
43	0.165729
44	0.241558
45	0.252262
46	0.399798
47	0.586928
48	0.851036
49	1.572102
50	1.245656
51	0.958978
52	0.251464
53	0.204472
54	0.364220
55	0.300178
56	0.178039
57	0.177791
58	0.250911
59	0.232509
60	0.145921
61	0.126760
62	0.128564
63	0.141068
64	0.153013
65	0.144609
66	0.107221
67	0.170729
68	0.167898
69	0.096529
70	0.050942
71	0.024704
72	0.014345
73	0.015775
74	0.033291
75	0.045561
76	0.072410
77	0.195089
⋮	
106	

(C) LD2-core (complexed)

Nucleotide Position	Relative Self-cleavage Levels
1	
⋮	
6	0.001473
7	0.00388
8	0.035427
9	0.076936
10	0.246933
11	0.656207
12	0.711707
13	0.951133
14	0.213634
15	0.198475
16	0.005693
17	0.054576
18	0.004939
19	0.009842
20	0.007937
21	0.03121
22	0.629579
23	1.890512
24	0.77078
25	0.291076
26	0.335198
27	0.132877
28	0.141725
29	0.183578
30	0.243749
31	0.058285
32	0.037203
33	0.120904
34	0.444934
35	0.366546
36	0.221611
37	0.163055
38	0.194632
39	0.108563
40	0.221114
41	0.808529
42	0.179884
43	0.199504
44	0.16693
45	0.305328
46	0.126038
47	0.00978
48	0.004443
49	0.002372
50	0.001134
51	2.79E-06
52	0.002467
53	0.017115
54	0.011677
55	0.008754
56	0.000249
57	0.000159
58	0.005881
59	0.002068
60	0.000952
61	0.004309
62	0.022678
63	0.06389
64	0.126041
65	0.205804
66	0.141211
67	0.170532
68	0.308481
69	0.637474
70	0.123865
71	0.076743
72	0.068669
73	0.080093
74	0.08131
75	0.106665
76	0.103481
77	0.091952
78	0.076336
79	0.052306
80	0.057136
81	0.043733
82	0.038206
83	0.040138
84	0.044485
85	0.042235
86	0.042943
87	0.072407
88	0.125225
89	0.168186
90	0.128331
⋮	
97	0.058693
98	0.189289
99	0.860742
100	1.36013
101	1.055232
102	1.578803
103	0.612122
104	0.145481
105	0.087883
106	0.081512
107	0.08773
108	0.09309
109	0.116757
110	0.157805
111	0.224963
112	0.409056
113	0.493022
114	0.269072
115	0.178872
116	0.089739
117	0.083439
118	0.109507
119	0.170251
120	0.341581
121	0.773714
122	2.08539
123	2.769699
124	0.447419
125	0.128304
126	0.146346
127	0.391248
128	0.264826
129	0.067765
130	0.002121
131	0.009574
132	0.038115
133	0.098375
134	0.273933
135	0.760003
136	1.892188
⋮	
188	

Figure S12. **Secondary structure analysis of the RTSL/LD2-core complex**. **(A)** Secondary structure of the RTSL/LD2-core complex with nucleotides coloured according to their relative in-line cleavage values, with red being frequently cleaved, green, cleaved at intermediate frequency, and black, infrequently cleaved. Nucleotides in grey represent the areas were relative in-line values could not be determined. The relative in-line probing data was obtained by quantifying the intensity of each band in the lane containing complexed RTSL and LD2-core RNAs (Figure 7C, lane 5; Figure 7A, lane 5) using the QuantityOne (Biorad) software, with background level subtracted. The values were normalized in the same manner as described in captions for Figure S9 and S10. The normalized self-cleavage values for RTSL and LD2-core were then mapped onto the RTSL/LD2-core complex, with the *trans*-interacting sequences in the RTSL/LD2-core complex deduced from the relative reactivities in the two RNAs. **(B), (C)** Tables showing nucleotide positions and their corresponding normalized in-line self-cleavage values of RTSL and LD2-core, respectively when complexed. Values for nucleotides 1-11 and 78-106 of RTSL and 1-5, 91-96, as well as, 137-188 of LD2-core could not be quantified. The relative in-line values are colour-coded according to the scale shown in panel (A).

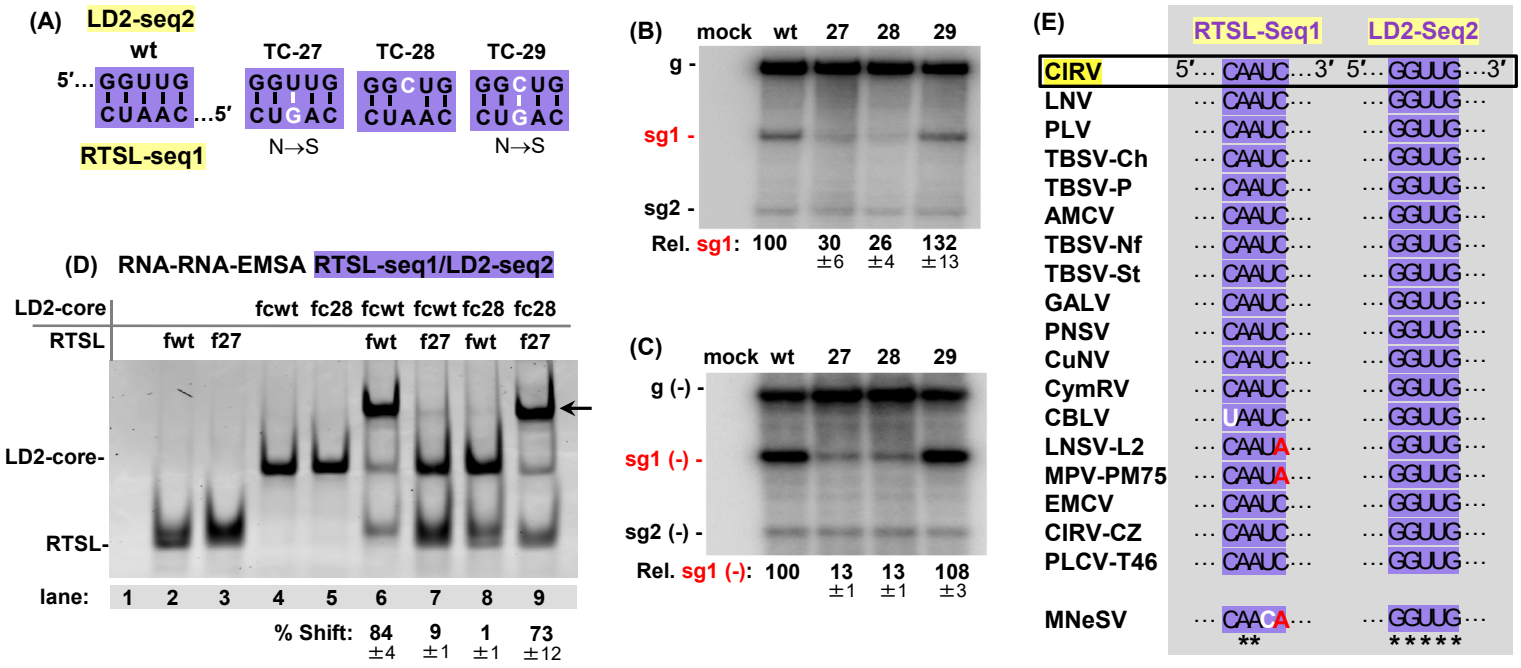

Figure S13. Functional analysis of the proposed second RTSL/LD2 interaction involving RTSL-seq1 and LD2-seq2. (A) Compensatory mutations introduced into the full-length CIRV genome in the proposed RTSL-seq1/LD2-seq2 LDRI (purple) are highlighted in white. Amino acid changes in the p95 ORF are indicated under each mutant. **(B)** Northern blot analysis of plus-strand RNAs isolated from protoplasts transfected with wt and mutant CIRV genomic RNAs shown in panel (A). Identities of the tested samples are indicated above the blot with the positions of positive-sense genome and sg mRNAs shown on the left. Average sg mRNA1 accumulation levels relative to that of the wt are provided below the blot with standard errors obtained from three independent experiments. **(C)** Northern blot analysis of minus-strand CIRV RNAs isolated from protoplasts transfected with wt and mutant CIRV genomic RNAs shown in (A). Identities of the tested samples are indicated above the blot and the positions of the minus-sense genome and sg mRNAs are shown on the left. Average minus-strand sg mRNA1 accumulation levels relative to that of the wt are provided below the blot with standard errors obtained from three independent experiments. **(D)** RNA-RNA EMSA results for the RTSL (106 nt) and LD2-core (188 nt) RNA fragments containing substitutions shown in (A). The contents of each lane are indicated above the native 8% polyacrylamide gel stained with ethidium bromide, with the fragment type shown on the far left. Lane 1 represents a mock lane containing only RNA binding buffer and glycerol. The black arrow on the right side of the image points to the position at which RTSL/LD2-core complex migrates. The percentages and standard errors of shifted LD2-core RNAs compared to the corresponding not-shifted LD2 RNAs are displayed below the gels obtained from three independent EMSA experiments. **(E)** Comparative sequence analysis of RTSL-seq1 and LD2-seq2 in the members of the Tombusvirus and Zeavirus genera. Red nucleotides represent substitutions that disrupt RTSL-seq1/LD2-seq2 interaction and the white nucleotide represents the substitution that maintains the interaction. Asterisks depict nucleotides that are 100% conserved among the compared viral sequences. See legend for Figure S4 for full names and accession numbers of the viral species.